International Journal of Microwave and Wireless Technologies, 2013, 5(1), 77–84.
doi:10.1017/S1759078712000827

RESEARCH PAPER

Optimization of a broadband directional gain microstrip patch antenna for X–Ku band application

ANUBHUTI KHARE AND RAJESH NEMA

In this paper, optimization of a microstrip patch antenna is presented. The optimization uses a genetic algorithm in the IE3D^{TM} Simulator. The optimization is done in several steps, first by changing the position of parasitic patches on the top layer, second by placing a feeding patch at the middle layer of geometry, and third by indirect coupling between the top and middle layer patches. Overall, we have performed many possible iterations and found appropriate geometry. From this appropriate geometry we have achieved maximum directional gain (6.2–8.8 dBi) over a 6 GHz bandwidth slot, 38% impedance bandwidth of the X-band and 14.8% impedance bandwidth of the Ku-band. The broadband frequency of operation is demonstrated by single geometry. The geometry of a single probe fed rectangular microstrip antenna incorporating a slot, gap coupled with a parasitic and an active patch on geometry, has been studied. We have investigated the height between active and parasitic patches as 0.0525λ and the height between parasitic patches itself as 0.0525λ. We have investigated the enhancement in maximum directional gain by stacking geometry with one active patch and two parasitic patches of different dimensions. This optimized antenna is used for X-band and Ku-band applications. The hardware validation and simulation results are matched to the proposed design.

Keywords: IE3D^{TM} Simulator, Maximum directional gain, Parasitic and active patch, Slit loading, X–Ku band, Genetic algorithm

Received 29 April 2012; Revised 8 December 2012

I. INTRODUCTION

An explosive growth of wireless radio communication systems is currently observed in the microwave band. In [1], a dual-layer micro-strip antenna working at 1.268 GHz was designed and analyzed. The bandwidth of the micro-strip antenna was 35 MHz, and the gain was 6 dB. In [2], a novel broadband microstrip patch antenna was proposed and studied. The antenna achieves broadband by adopting a bilayer patch for coupling; a capacitive metal-wafer is introduced at the top of the feeding probe to counteract the inductance caused by the probe. In addition, Minkowski fractal-patch structure was applied in antenna design to realize its miniaturization. The reflection coefficient is lower than −10 dB at 3.33–4.0 GHz and the impedance bandwidth is 18.3%. Moreover, antenna gain is stable and higher than 6.5 dBi. In [5], wide-band dual-polarized microstrip antennas were studied. The experimental results showed that an impedance bandwidth (SWR ≤ 2) of 33.24% and a peak gain of 8.44 dBi (at 2.11 GHz) were obtained. They were designed originally for the triple service band. In [6], a stacked microstrip antenna with aperture coupling feeding as the individual radiator of the wide band antenna array was studied. With adjusted parameters, it exhibits a broad impedance bandwidth (VSWR ≤ 2) of about 27% (8.8–11.6 GHz).

In [7], new electromagnetic coupling fed low profile broad-band high gain E-shaped microstrip antennas (MSA) were proposed for high speed wireless networks in IEEE 802.11a and standards. The proposed antenna uses an E-shaped microstrip patch covered by a radome and fed by an electromagnetically coupled strip. To validate this concept, a single antenna element and a sub-array were designed, built, and measured. The measured results indicate that the element and the sub-array cover the band from 4.8 to 6.0 GHz (return loss <-10 dB) and produce a gain of 8 and 11 dBi, respectively. In [8], a simple bandwidth enhancement method for low profile E-shaped patch antennas was presented. By introducing a distributed LC circuit to the E-shaped patch antenna, a new resonant frequency close to that of the E-shaped patch was obtained; measured results show that the designed low profile antenna achieved an impedance bandwidth over 9% for VSWR < 2. In paper [12], a multiple slot microstrip patch antenna for wireless communication was presented, inverted microstrip patch antenna, direct probe feed technique, and the novel multiple shaped patch is used in antenna design. The multi-slotted microstrip patch antenna achieved a fractional bandwidth of 27.89% (1.82–2.41 GHz) at 10 dB return loss. Microstrip antennas were found to be favorable because they were (1) low profile and (2) inexpensive to manufacture and compatible with monolithic microwave integrated circuit designs (MMIC). However, they also had drawbacks such as (a) low efficiency

Department of Electronics and Communication, University Institute of Technology RGPV, Bhopal, India
Corresponding author:
R. Nema
Email: rajeshnema2010@rediffmail.com

and (b) narrow impedance bandwidth. The input impedance of MSDA depends on its geometrical shape, dimension, and feed type. Therefore, antenna input impedance is an important design parameter that controls the radiated power and the impedance bandwidth. In most applications, bandwidth limitations occur due to an impedance mismatch. In this respect, a microstrip antenna has narrow bandwidth because of heavy reactance. As microstrip antennas have found a wide variety of application areas, a number of techniques have evolved to improve their limited bandwidth. A straightforward application to improve the bandwidth is by increasing the thickness of the substrate supporting the microstrip patch. However, limitations exist with the ability to effectively feed the patch on a thick substrate and the radiation efficiency can degrade with increasing substrate thickness. Techniques for overcoming these band limiting problems can be achieved by using parasitic term elements, external matching, and separating the feed and antenna. The proximity coupling method uses an impedance matching stub connected to the feed line achieving 13% bandwidth. A broadband rectangular patch antenna with a pair of wide slits of near resonance frequency improves to 24% bandwidth. Bandwidths of 10–12% can be obtained using the passive coplanar matching network. However, the gain and radiation pattern is distorted. Using an aperture-coupled antenna, bandwidths larger than 20% are achieved.

II. PROCEDURE FOR OPTIMIZATION

In this paper, we present an optimized microstrip patch antenna for achieving large gain over large bandwidth, using change in the position of parasitic patches on the top layer.

A) Optimization by placing two parasitic patches on the top layer as shown in Fig. 1

The proposed model of optimization Section A is shown in Fig. 3 and 3D view of Proposed Model of optimization Section A is shown in Fig. 2. We optimized spacing S between top patches, using two parasitic patches on the left side of the geometry, and verified the result for each spacing and appropriate position. After a number of iterations, appropriate spacing $S = 2\lambda$ was achieved.

We optimized the following points and achieved an appropriate value.

a. Slot loaded on parasitic patch.
b. $\Delta = 3$ mil air gap between layers.
c. Whole geometry consists of the layer glass epoxy PCB and air gap (FR-4–air–FR-4).
d. Total height of geometry is 121 mil (from a ground plan to top layer).
e. Spacing between parasitic patches is $S_1 = 62$ mil.
f. Spacing between active and parasitic patches is $S = 23.62$ mil (0.02λ).
g. Middle layer consists of patch dimension $L \times W = 411 \times 446$ mil^2.
h. Top layer consists of multilayer parasitic patches of the same dimension $L_1 \times W_1 = 100 \times 150$ mil^2.
i. Optimization by changing the position of top parasitic patches.

The top layer dimension of optimization section A is shown in Fig. 4.

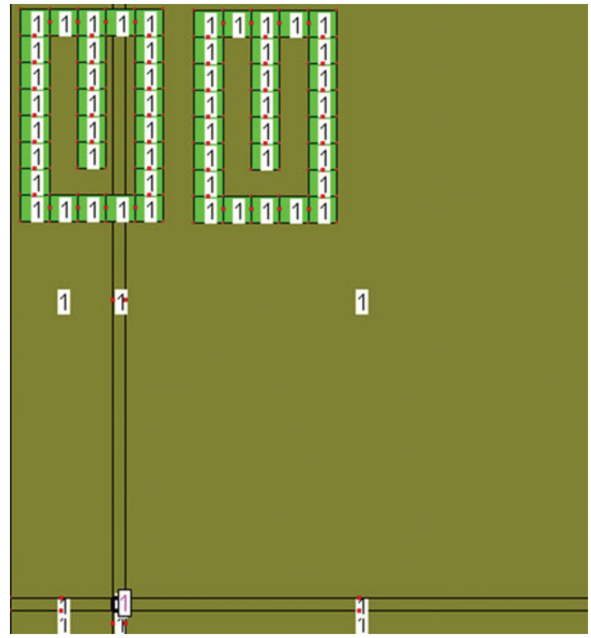

Fig. 1. Proposed design of Section II(A).

From the first optimization section, we achieved optimal directional gains of 6.4–8 dBi over a 5.9 GHz bandwidth slot (8.5–14.5 GHz). The first optimization section includes U-slots on the top patches for impedance matching over a large bandwidth, the gap spacing between top patches is $S = 2\lambda$, the total height of the proposed antenna is 121 mil by using a multilayer concept and the air gap between the top and bottom layers substituted the 411×446 mil^2 patch on the middle layer of geometry and the feed probe connected to the middle layer. The current density on the top parasitic patches depends on the geometry of top patches 100×150 mil^2, cutting slot length, width of the slot, and the gap between parasitic patches. We have observed strong coupling between top patches and achieved optimal gains. The results of this optimization are shown in Figs 5–7.

We have achieved VSWR ≤ 2 over a 5.9 GHz impedance bandwidth (8.5–14.5 GHz), and -10 dB impedance bandwidth over a 5.9 GHz bandwidth slot. However, in terms of directional gain and bandwidth, we require further modifications in the result so that the position of parasitic patches is changed on the top layer and the observed results achieve 34% impedance bandwidth of the X-band and 13.4% impedance bandwidth of the Ku-band as shown in Fig. 5.

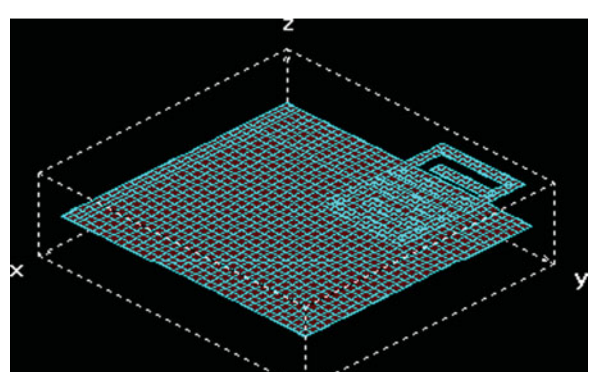

Fig. 2. 3D view of Section II(A).

https://doi.org/10.1017/S1759078712000827 Published online by Cambridge University Press

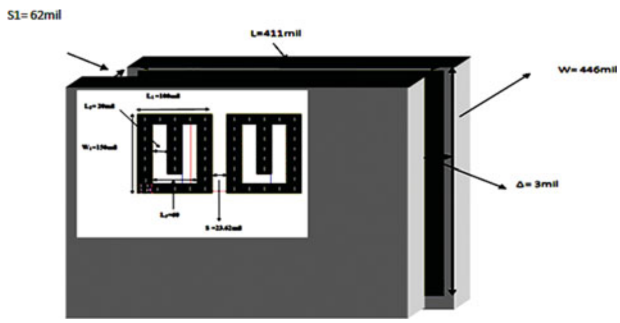

Fig. 3. Proposed model of Section II(A).

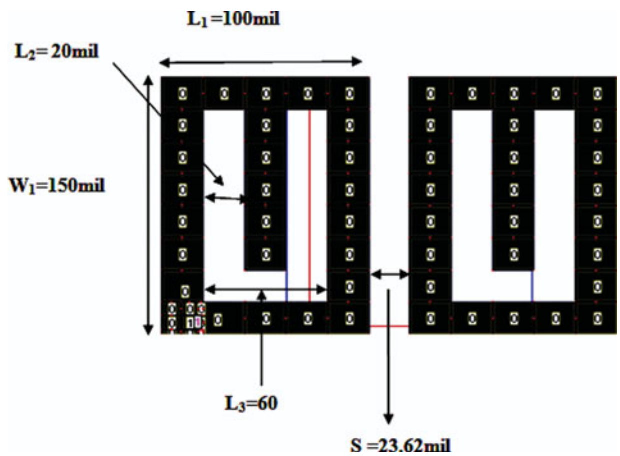

Fig. 4. Front view of optimization design for $S = 2\lambda$.

B) Effect of two parasitic patches: one at the left side bottom corner and another at the right side top corner

For enhancing the flat gain curve over large bandwidth, we require further modifications in the previous design so that we can arrange one parasitic patch at the right side top corner and the second patch at the left side bottom corner

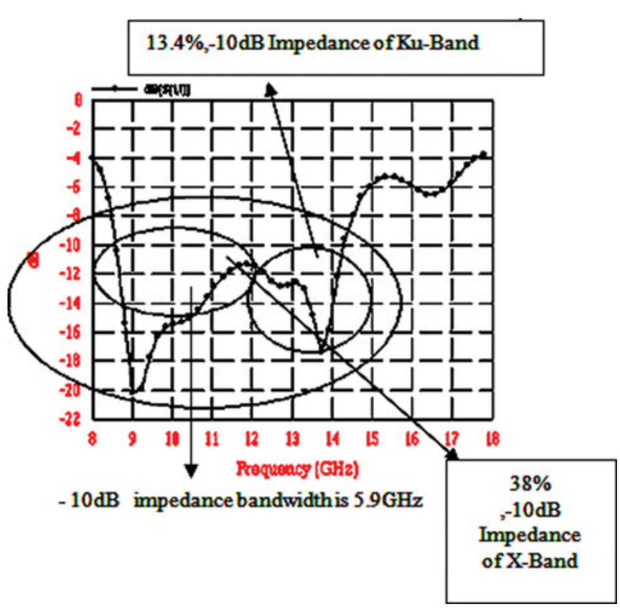

Fig. 5. Return losses versus frequency.

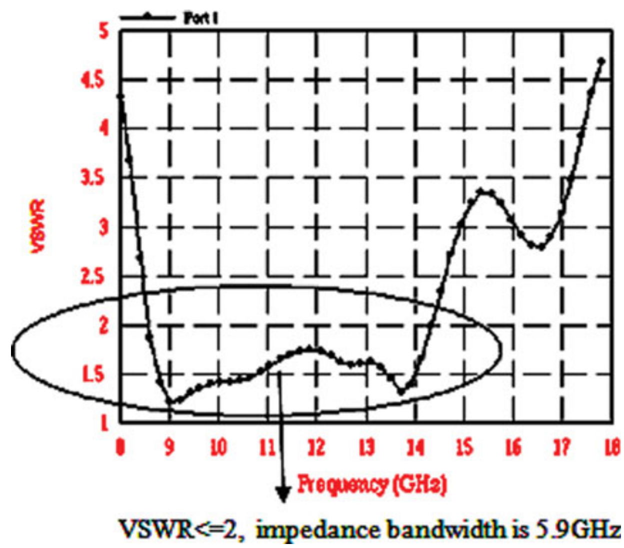

Fig. 6. VSWR versus frequency.

as shown in Fig. 8. 3D View of Section B is shown in Fig. 9. From this arrangement, the left side patch provides impedance bandwidth for the lower edge of the frequency and the topside patch provides impedance bandwidth for the higher edge of the frequency due to which we have achieved a 5.7 GHz broad bandwidth slot. From optimization section B reduced mismatching loss, ohmic loss and circular polarization loss. Losses are reduced due to removing most of copper and placing two U-Slots on the cross arrangement on top layer. Overall, we achieved 6.2–8.8 dBi over a broad bandwidth 5.7 GHz (8.5–14.5 GHz). All results shown in Figs 10–12 achieved VSWR ≤ 2 over a 5.7 GHz bandwidth slot, -10 dB impedance bandwidth up to 5.7 GHz and 38% impedance bandwidth of the X-band and 12.77% impedance bandwidth of the Ku-band as shown in Fig. 10.

C) Effect of two parasitic patches: one at the left side of the top corner and another at the right side of the bottom corner

In section C, we have arranged one parasitic at the right side bottom corner and second at the left side top corner shown in

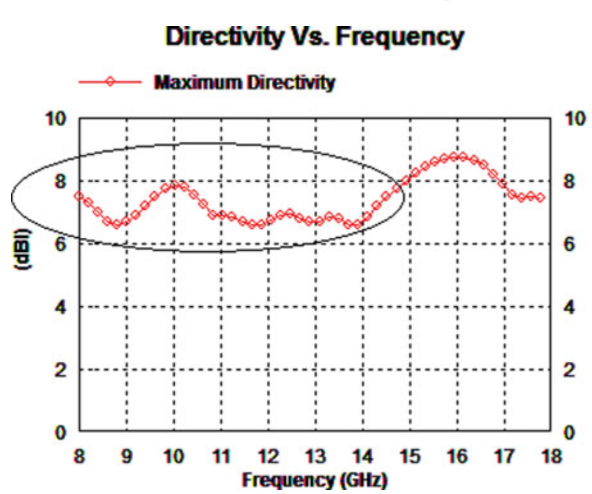

Fig. 7. Directivity versus frequency.

https://doi.org/10.1017/S1759078712000827 Published online by Cambridge University Press

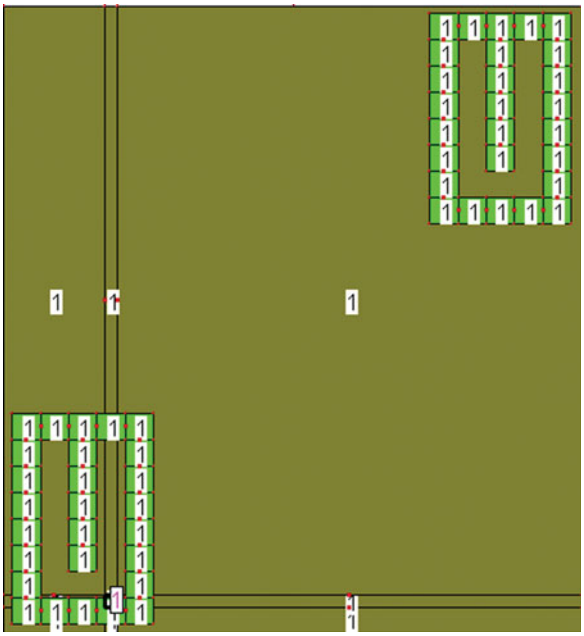

Fig. 8. Modified design for Section II(B).

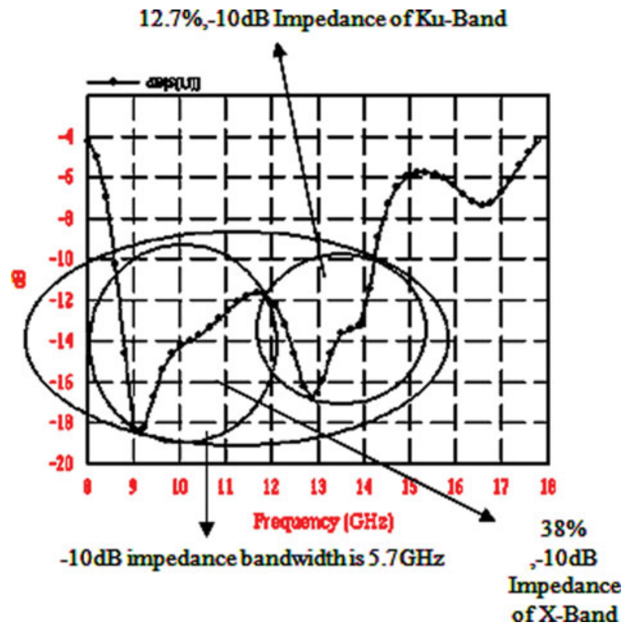

Fig. 10. Return losses versus frequency for Section II(B).

Fig. 13 and 3D View of Section C is shown in Fig. 14. From this optimization, we achieved a 5.8 GHz broad bandwidth slot, the left side parasitic patch provided impedance bandwidth for the lower edge of the frequency and the topside parasitic patch provided impedance bandwidth for the higher edge of the frequency. The position of patches reduced surface loss, cross polar loss; achieved more flat directional gains 6–8 dBi over a broad bandwidth of 5.8 GHz (8.5–14.5 GHz) shown in Fig. 17, achieved VSWR ≤ 2 over a 5.8 GHz bandwidth slot, −10 dB impedance bandwidth up to a 5.8 GHz slot of bandwidth. All the results are shown in Figs 15–17; we achieved 38% impedance bandwidth of the X-band and 13.36% impedance bandwidth of the Ku-band as shown in Fig. 15.

D) Effect of four parasitic patches: two at the top corner and another two at the bottom corner

We arranged two parasitic patches at the right side corners and two other parasitic patches at the left side corners as shown in Figs 18 and 19. From this arrangement, we achieved a 6 GHz broad bandwidth. The position of the patches reduces surface loss, cross polar loss, and ohmic loss. We achieved a very high flat directional gain of 6.2–8.8 dBi over a broad bandwidth of 6 GHz (8.5–14.5 GHz) as shown in Fig. 20. All the results are shown in Figs 20–22; we achieved 38% impedance bandwidth of the X-band and 14.8% impedance bandwidth of the Ku-band as shown in Fig. 18.

We have further discussed the method of fabrication. For the fabrication, FR-4 and air are used; firstly by designing the layout in AutoCAD software, etching is completed using ferric-chloride acid, and for feeding the SMA Connector is used. The fabricated proposed antenna is shown in Fig. 23.

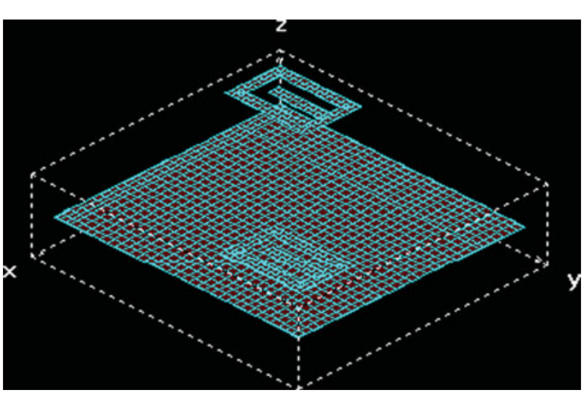

Fig. 9. 3D view of Section II(B).

III. RESULTS AND DISCUSSION

We have focused on optimal directional gain and broad bandwidth. For achieving these outcomes, we have used the genetic

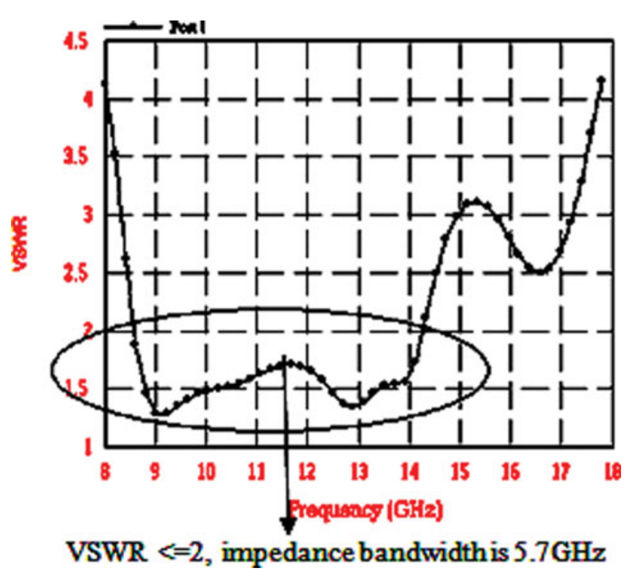

Fig. 11. VSWR versus frequency for Section II(B).

https://doi.org/10.1017/S1759078712000827 Published online by Cambridge University Press

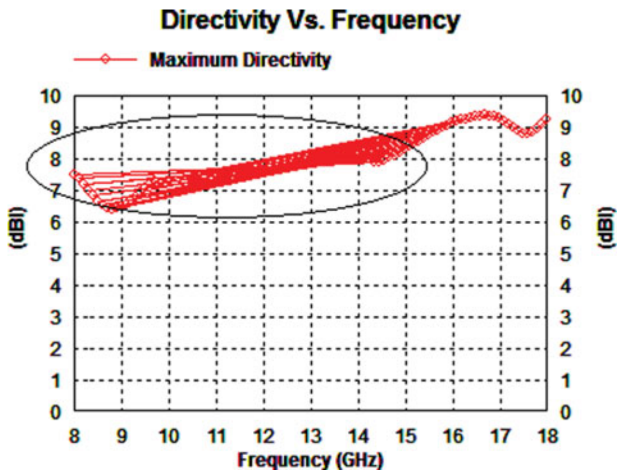

Fig. 12. Directivity versus frequency.

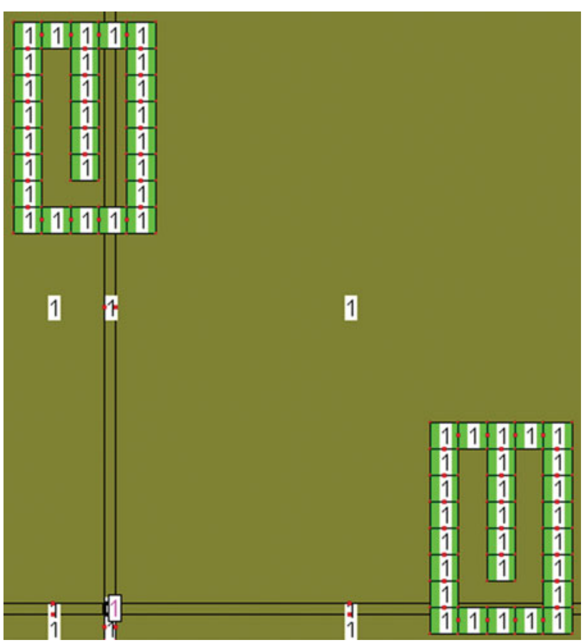

Fig. 13. Modified design for Section II(C).

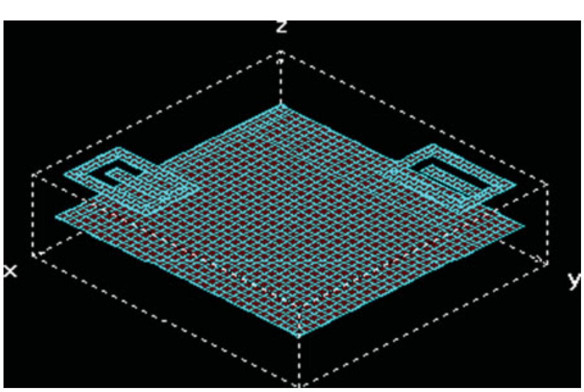

Fig. 14. 3D view of Section II(C).

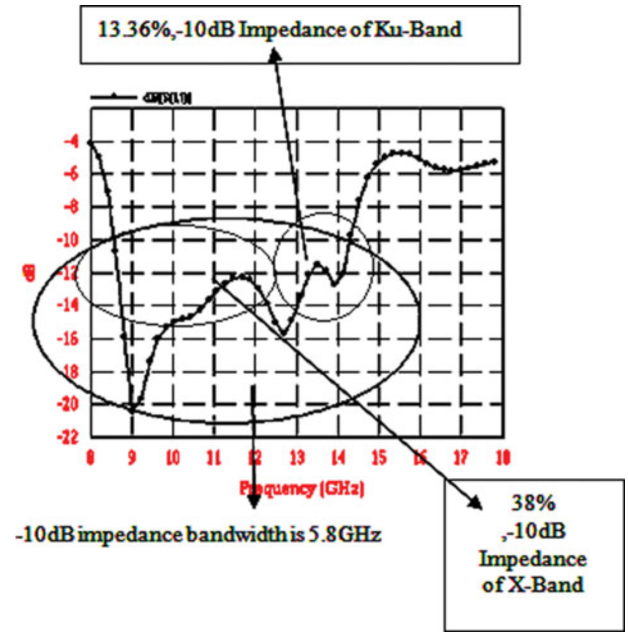

Fig. 15. Return loss versus frequency for Section II(C).

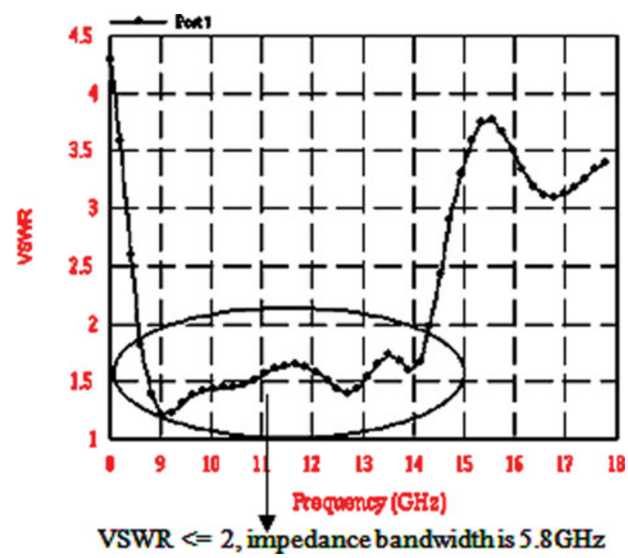

Fig. 16. VSWR versus frequency for Section II(C).

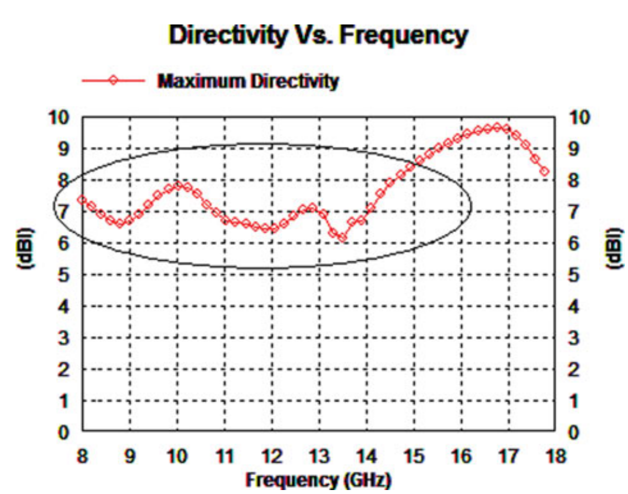

Fig. 17. Directivity versus frequency.

https://doi.org/10.1017/S1759078712000827 Published online by Cambridge University Press

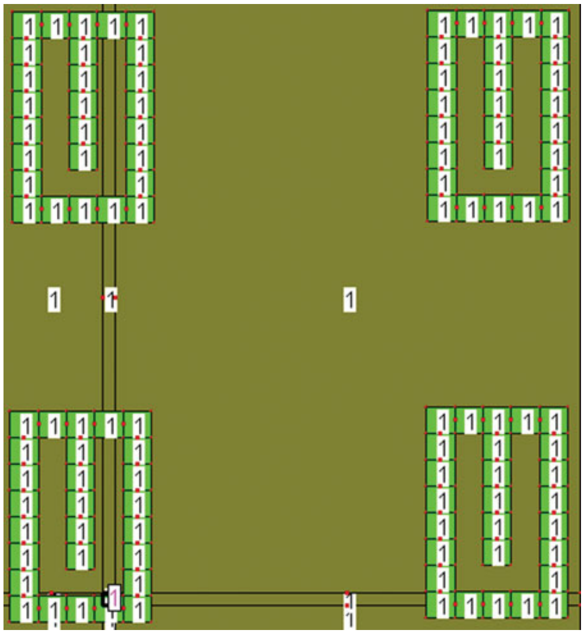

Fig. 18. Modified design for Section II(D).

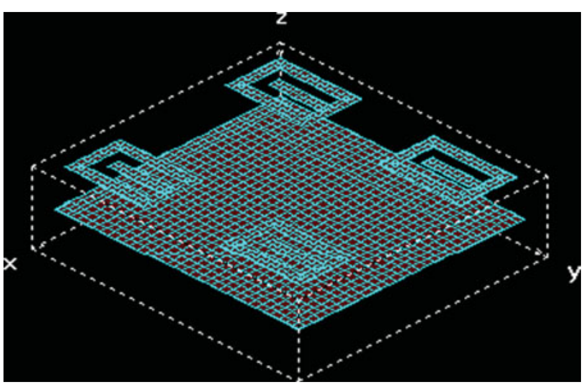

Fig. 19. 3D view of Section II(D).

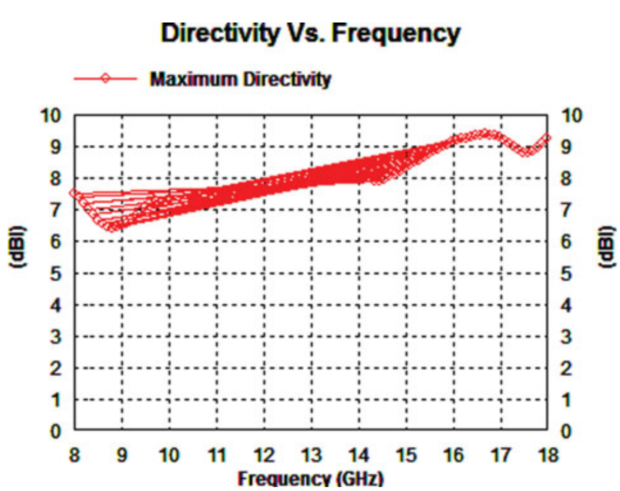

Fig. 20. Directivity versus frequency.

algorithm on an IE3D^{TM} Simulator. The impedance frequency bandwidth of a microstrip antenna depends primarily on the thickness, the dielectric permittivity of the substrate, position, and dimension of the parasitic patch on the top layer. We have

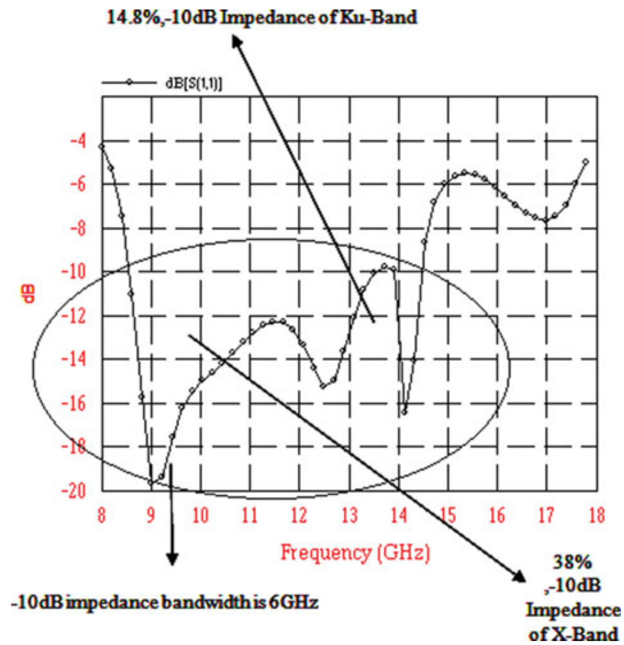

Fig. 21. Return loss versus frequency for Section II(C).

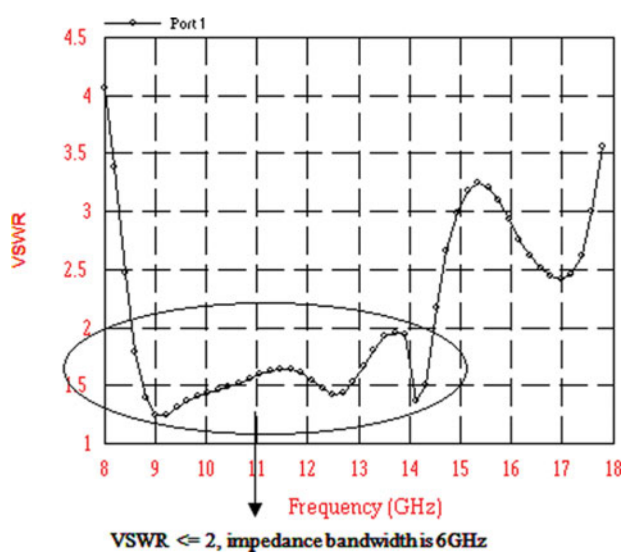

Fig. 22. VSWR versus frequency for Section II(C).

analyzed four cases. From the first case (Section II(A)) we achieved 5.9 GHz impedance bandwidth, from the second case (Section II(B)) we achieved 5.7 GHz impedance bandwidth, from the third case (Section II(C)) we achieved 5.8 GHz impedance bandwidth, and from the fourth case (Section II(D)) we achieved 6 GHz impedance bandwidth. All geometry consists of a parasitic array concept. We have studied stack geometry with a number of active and parasitic patches for enhancing the maximum directional gain and reduction in surface wave, cross polarization loss. We have achieved good impedance matching due to all aspects of modeling and achieved maximum directional gains of 6.2–8.8 dBi from Section II(D). All optimization section results are shown in Table 1.

https://doi.org/10.1017/S1759078712000827 Published online by Cambridge University Press

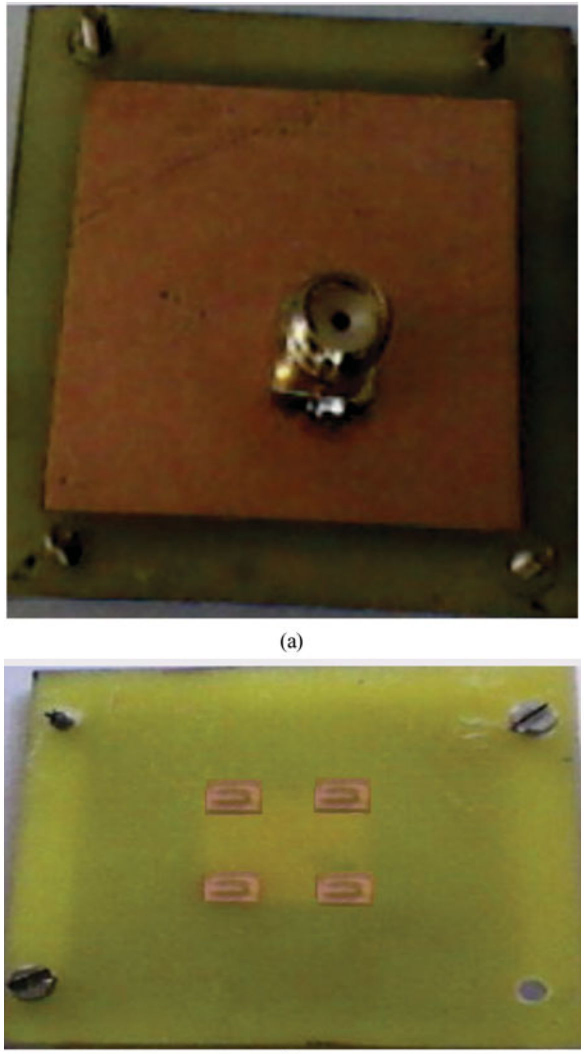

(a)

(b)

Fig. 23. (a) Bottom view of fabricated proposed antenna. (b) Top view of fabricated proposed antenna.

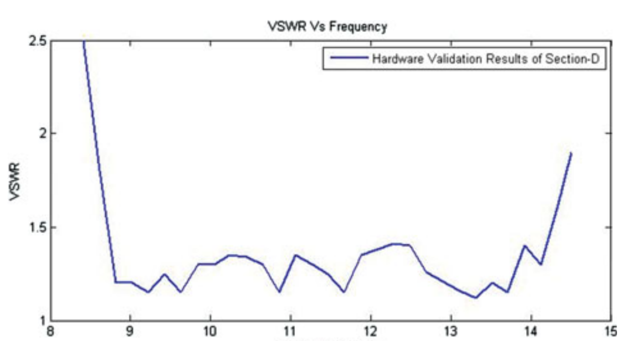

Fig. 24. Hardware validation of fabricated antenna.

A) Hardware's validation results

The hardware validation and IE3D^{TM} Simulator results are shown in Table 1. Hardware validation results are the same as IE3D^{TM} Simulator results is shown in Fig. 24.

Table 1. VSWR versus frequency.

Frequency (GHz)	VSWR for Section II(A)	VSWR for Section II(C)	VSWR for Section II(B)	VSWR for Section II(D)	Hardware validation VSWR results of Section II(D)
8.408	2.67	2.616	2.5088	2.468	2.5
8.612	1.867	1.88	1.816	1.778	1.8
8.816	1.408	1.454	1.381	1.389	1.2
9.02	1.214	1.277	1.208	1.232	1.2
9.224	1.233	1.277	1.231	1.24	1.15
9.429	1.296	1.342	1.309	1.304	1.25
9.633	1.357	1.407	1.373	1.363	1.15
9.837	1.393	1.455	1.413	1.404	1.3
10.04	1.407	1.483	1.431	1.432	1.3
10.24	1.413	1.5	1.438	1.454	1.35
10.45	1.429	1.516	1.449	1.481	1.34
10.65	1.466	1.543	1.476	1.516	1.3
10.86	1.523	1.58	1.517	1.555	1.15
11.06	1.586	1.621	1.563	1.593	1.35
11.27	1.646	1.66	1.603	1.623	1.3
11.47	1.696	1.691	1.632	1.639	1.25
11.67	1.73	1.706	1.642	1.605	1.15
11.88	1.742	1.693	1.626	1.544	1.35
12.08	1.724	1.645	1.579	1.47	1.38
12.29	1.676	1.559	1.504	1.418	1.41
12.49	1.618	1.453	1.426	1.432	1.4
12.69	1.585	1.365	1.39	1.522	1.26
13.1	1.594	1.337	1.433	1.658	1.16
13.31	1.611	1.379	1.538	1.803	1.121
13.51	1.571	1.456	1.54	1.916	1.2
13.71	1.443	1.521	1.722	1.952	1.15
13.92	1.311	1.537	1.68	1.932	1.4
14.12	1.383	1.548	1.596	1.355	1.3
14.33	1.651	1.726	1.656	1.494	1.6
14.5	1.98	2	1.971	2	1.9

IV. CONCLUSION

From the optimization of four sections (Sections II(A)–II(D)) in the IE3D^{TM} Simulator using the genetic algorithm, we obtained appropriate geometry. The Geometry Section II(D) reported a 6 GHz S11 < -10 dB impedance bandwidth slot; we achieved 38% impedance bandwidth of the X-band and 14.8% impedance bandwidth of the Ku-band. The optimization section has two parasitic patches, one at the top corner of the left side and one at the bottom corner of the right side, and has reported 5.9 GHz $S_{11} < -10$ db impedance bandwidth slots. Overall we have been concluded that the geometry has two parasitic patches in the left side corner and two parasitic patches in the right side corner is optimum. The optimization section of four parasitic patches (Section II(D)) provided a high flat gain response of 7.5 dB, over a 6 GHz bandwidth slot (8.5–14.5 GHz). We performed optimization in four steps, by changing the position of parasitic patches on the top layer, and analyzed results on the IE3D^{TM} Simulator. The appropriate four parasitic patches on top layer antenna design are useful for X–Ku band application, used as a Satellite and Radar antenna at the X–Ku band. The hardware validation and simulation results are matched.

ACKNOWLEDGEMENT

This work was supported by Lambda Microwave Pvt. Ltd for hardware validation.

REFERENCES

[1] Xuzhe, L.; Hua, S.; Huaiwu, Z.; Zhiyong, Z.: Design of broadband dual-layer microstrip antenna, in Mechanic Automation and Control Engineering (MACE), 2011 Second Int. Conf. on Digital Object Identifier Publication, 2011, 6422–6425.

[2] Guanlong, H. et al.: Bilayer miniature broadband microstrip patch antenna with Minkowski Fractal, in Microwave Conf. Proc. (CJMW), 2011 China-Japan Joint Publication, 2011, 1–4. ISBN: 978-1-4577-0625-7.

[3] Latif, S.I.; Shafai, L.; Shafai, C.: Gain and efficiency enhancement of compact miniaturized microstrip antennas using multi-layered laminated conductors, IET Microw. Antennas Propag., **5** (2011), 402–411.

[4] Yuxiang, Z.; Su, Y.; Bofan, S.; Lei, S.: Experimental studies of microstrip-fed slot antennas for harmonic suppression, in 2011 IEEE Int. Conf. on Signal Processing, Communications and Computing (ICSPCC), 14–16 September 2011, 1–3. ISBN: 978-1-4577-0893-0.

[5] Jeon, J.S.: Design of wideband dual-polarized microstrip antennas, in Proc. XXX General Assembly and Scientific Symposium of the International Union of Radio Science (URSI GASS 2011), Istanbul, Turkey, August 13–20, 2011, 1–4. ISBN: 978-1-4244-5117-3.

[6] Zhang, F.; Zhang, F.-S.; Lin, C.; Zhao, G.: BROADBAND MICROSTRIP patch antenna array using stacked structure, in 2010 Int. Conf. on Microwave and Millimeter Wave Technology (ICMMT), 8–11 May 2010, 388–391. Springer-Verlag, York. ISBN: 978-1-4244-5705-2.

[7] Bhatnagar, M.: For high-speed wireless network's broadband and high-gain E-shaped microstrip antennas, In ELECTRO '09. Int. Conf. on Emerging Trends in Electronic and Photonic Devices and Systems, 22–24 December 2009, 300–302. ISBN: 978-1-4244-4846-3.

[8] Yikai, C.; Shiwen, Y.; Zaiping, N.: Bandwidth enhancement method for low profile E-shaped microstrip patch antennas, in IEEE Trans. Antennas Propag., **58** (7) (2010), 2442–2447.

[9] Latif, S.I.; Shafai, L.; Shafai, C.: Ohmic loss reduction and gain enhancement of microstrip antennas using laminated conductors, in 13th Int. Symp. on Antenna Technology and Applied Electromagnetics and the Canadian Radio Science Meeting, 2009, ANTEM/URSI 2009, 15–18 February 2009, 1–4. ISBN: 978-1-4244-2979-0.

[10] Cheng, Q.; Zhou, X.Y.; Zhou, B.; Xu, S.; Cui, T.J.: A superstrate for microstrip patch antennas, In 2008 Int. Workshop on Metamaterial, 9–12 November 2008, 382–384. ISBN: 978-1-4244-2608-9.

[11] Islam, M.T.; Misran, N.; Shakib, M.N.; Yatim, B.: Wideband Stacked Microstrip Patch Antenna for Wireless Communication, in ISPA '08. Int. Symp. on Parallel and Distributed Processing with Applications, 2008, 10–12 December 2008, 547–550. ISBN: 978-0-7695-3471, 8.

[12] Jay nthy, T.; Sugadev, M.; Ismaeel, J.M.; Jegan, G.: Design and simulation of Microstrip M-patch antenna with double layer. Int. Conf. on Recent Advances in Microwave Theory and Applications, 2008. MICROWAVE IEEE 2008, ISBN: 978-1-4244-2690-4. 230–232.

[13] Ray, K. P.; Ghosh, S.; Nirmala, K.: Compact broadband gap-coupled microstrip antennas, in Proc. IEEE Antennas and Propagation Society Int. Symp., July 2006, 3719–3722.

[14] Li, X.; Li, C.: Design of high gain multiple U-slot microstrip patch antenna for wireless system Bottom of Form, in 2010 Int. Conf. on Computational Problem-Solving (ICCP), 3–5 December 2010, 256–259. ISBN: 978-1-4244-8654-0.

Dr Anubhuti Khare (BE, MTECH, Ph.D.) is a Professor in the Electronics and Communication department, UIT RGPV Bhopal. She has published 50 papers in international journals. She has guided many theses for PG students and Ph.D. scholars. She has 20 years of teaching experience at the PG and UG level.

Rajesh Nema (BE, MTECH, pursuing a Ph.D.) is a Ph.D. scholar at UIT RGPV Bhopal. He has published 10 papers in international journals.

https://doi.org/10.1017/S1759078712000827 Published online by Cambridge University Press